AAE 5626: Orbital Mechanics for Engineers

Mrinal Kumar©

October 15, 2022

Interplanetary Mission Design: Patched Conics

The full-blown problem of interplanetary mission design is extremely complex because it involves the motion of a spacecraft under the gravitational influence of the sun as well as *all the other planets it "flies close to"*, in particular the Earth and the target planet. In other words, the design of an interplanetary trajectory is an $n-$body problem, where the value of "n" depends on the nature of the mission. However, due to the large size of the solar system, it is possible to decompose this complex problem into a set of multiple two-body problems and stitch the resulting trajectories together to obtain the overall solution. This is a surprisingly accurate first approximation and we will look at this so-called "patched conic" approach in significant detail.

- Essentially, the patched conic technique decomposes the overall mission design into three two-body problems, each involving the design of a single conic section described below:

  1. **Departure hyperbola:** This part of the mission takes place "close to the Earth", where the influence of the Sun and the target planet (e.g. Mars) are negligible. In the context of the two-body problem, the central object is the Earth and the secondary object is the spacecraft. The designed conic section is a hyperbola that allows the spacecraft to escape the confines of the Earth.
  2. **Cruise ellipse:** This part of the mission takes place in the "playing fields" of the solar system, when the spacecraft is sufficiently far from both the originating planet (Earth) and the target planet (e.g. Mars). Thus the two bodies involved are the spacecraft and the Sun. The conic section is an ellipse with the Sun at the focus.
  3. **Arrival hyperbola:** In this final phase, the spacecraft has reached sufficiently close to the target planet for us to safely ignore the effects of the Sun and Earth. The spacecraft and the target planet form the two-body system and the former approaches the latter on an incoming hyperbolic trajectory. Of course, if nothing else is done, the spacecraft will reach its point of closest approach to the target on its incoming hyperbola and then fly away. Therefore, very close to the planet (near the periapsis) a "capture maneuver" must be performed to get the spacecraft firmly in control of the target planet.

- In each of the three two-body problems described above, one of the two bodies involved is the spacecraft. It basically travels from the regime of the Earth to the regime of the Sun to the regime of the target planet.

- The three conic sections are patched together to form the composite mission design. The large distances involved in the solar system make the above described decoupling a fairly accurate approximation. Each object has its own "sphere of influence" inside which it can be assumed to exert the dominant force on the spacecraft. Fig.(1) illustrates the idea of patched conicss. The target planet is Mars. Earth at the time of launch and Mars at the time of arrival are shown, along with a view of their spheres of influence (shown highly exaggerated).

- The "sphere of influence" is actually a very well developed idea. In order to make the patched conics method to work, we must precisely define the size of this sphere because it serves as the boundary on which the patching points between two neighboring conics lie (points $P1$ and $P2$ in Fig.(1)). There exist many definitions of the sphere of influence. The key is to pick one definition and stick with it throughout the design process.

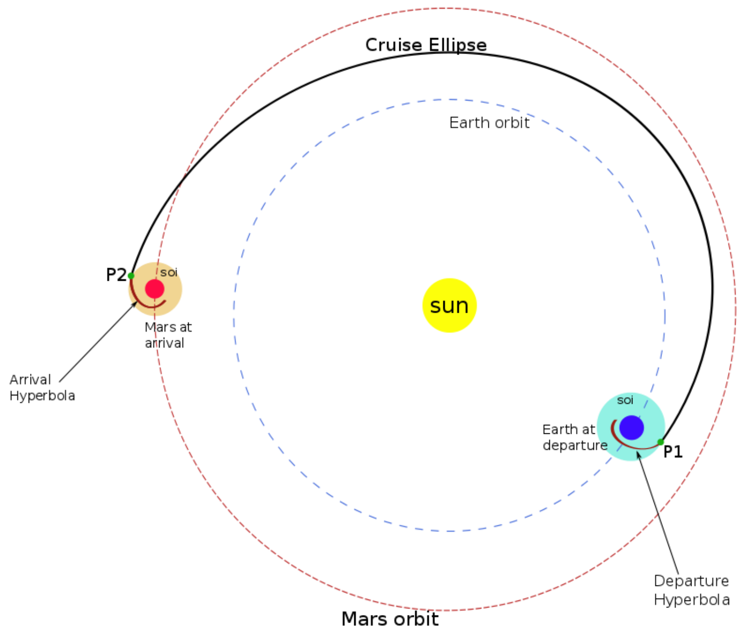

Figure 1: The *patched conic approach* to interplanetary mission design.

Sphere of Influence

Before designing interplanetary missions by patching conic sections, we must define the region of validity of the individual conics. This leads to the idea of a sphere of influence (SOI), which essentially, is the region surrounding a central object inside which it can safely be assumed to be the dominant force of gravity acting on the spacecraft. The "sphere of influence" is the justification behind the decoupling of the complex n-body problem into multiple two-body problems.

- There exist many definitions of an SOI. They are <u>not</u> all equivalent and lead to different estimates of the size of this region. We will use the definition given by Laplace (it is the most widely used). Consider the *three-body problem* shown in Fig.(2). In this picture, there are three objects:

  i. m: This is the "small object", and in our case, the spacecraft. Practically speaking, this object does not influence the motion (specifically, the acceleration) of the other two "larger" objects.

  ii. m_s: This is the biggest of the three objects (mass-wise). This object has the most dominant gravitational force among all three. In the present context, m_s is the sun.

  iii. m_p: This is an intermediate object, and in our case, the planet. We are interested in determining the extent of the region close to m_p inside which the influence of m_s on m can be safely ignored. This region will be defined as the sphere of influence of m_p. The small object m has no sphere of influence of its own. It is simply at the mercy of m_s and m_p!

- <u>Very important:</u> The concept of "sphere of influence" is understood in the *relative sense*. It is meaningless to talk of the SOI of an object in the absolute sense. For example, in Fig.(2) the are concerned with finding the SOI of m_p *relative to* m_s.

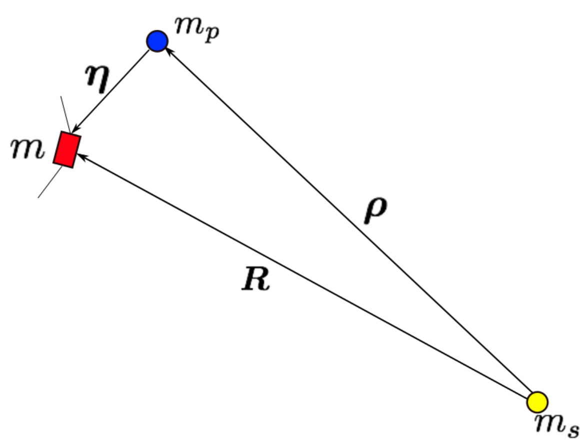

Figure 2: The geometry behind the *sphere of influence*.

- Let us now look at the geometry of Fig.(2). We see that

$$\mathbf{R} = \boldsymbol{\rho} + \boldsymbol{\eta} \tag{1}$$

We expect the SOI radius to be *much smaller* than $\mathbf{R}$. Because only then the object m is far enough from m_s and close enough to m_p for the latter to act as the dominant force. Therefore, we expect

$$\frac{\eta}{R} \ll 1 \tag{2}$$

Equivalently,

$$R \approx \rho \tag{3}$$

- Let us consider the inertial motion of the small object, m. Consider an inertial frame attached to m_s (this is OK: why?). We have:

$$m\ddot{\mathbf{R}} = \mathbf{F}_{m/m_p} + \mathbf{F}_{m/m_s} \tag{4}$$

where, $\mathbf{F}_{m/m_p}$ is the gravitational force on m exerted by the intermediate object m_p and $\mathbf{F}_{m/m_s}$ is the gravitational force on m due to m_s. Following Newton's universal law of gravitation,

$$\mathbf{F}_{m/m_p} = \frac{Gmm_p}{\eta^3}(-\boldsymbol{\eta}) \tag{5a}$$

$$\mathbf{F}_{m/m_s} = \frac{Gmm_s}{R^3}(-\mathbf{R}) \tag{5b}$$

Using Eqs.(5) in Eq.(4),

$$\ddot{\mathbf{R}} = -\frac{Gm_p}{\eta^3}\boldsymbol{\eta} - \frac{Gm_s}{R^3}\mathbf{R} \tag{6}$$

Now consider the following line of reasoning:

a. m_s is the most dominant object.

b. Eq.(6) is the motion of m as seen from an inertial frame fixed at m_s.

c. Therefore, we must view the acceleration of m *due to* m_s as the "primary acceleration", and the acceleration of m *due to* m_p as the "secondary" or a "disturbing acceleration".

Thus, define

$$\mathbf{a}_s \triangleq -\frac{Gm_s}{R^3}\mathbf{R} = \text{"primary"} \tag{7a}$$

$$\mathbf{a}_{d_p} \triangleq -\frac{Gm_p}{\eta^3}\boldsymbol{\eta} = \text{"disturbance"} \tag{7b}$$

In terms of the above,

$$\ddot{\mathbf{R}} = \mathbf{a}_s + \mathbf{a}_{d_p} \tag{8}$$

such that the magnitudes are: $a_s = Gm_s/R^2$ and $a_{d_p} = Gm_p/\eta^2$. We can now compare these magnitudes by looking at their ratio:

$$\frac{a_{d_p}}{a_s} = \frac{m_p}{m_s}\left(\frac{R}{\eta}\right)^2 \tag{9}$$

- Next, we will attempt to study the motion of m with respect to m_p, i.e. we are interested in $\ddot{\boldsymbol{\eta}}$. To get there, we first need $\ddot{\boldsymbol{\rho}}$:

$$m_p\ddot{\boldsymbol{\rho}} = \mathbf{F}_{m_p/m} + \mathbf{F}_{m_p/m_s} \tag{10}$$

which is nothing but the equation of motion of the mass m_p with respect to the inertial frame attached at m_s. This equation is exactly like Eq.(4) and the terms in the RHS must be interpreted in the same way:

$$\mathbf{F}_{m_p/m} = \frac{Gmm_p}{\eta^3}(+\boldsymbol{\eta}) \tag{11a}$$

$$\mathbf{F}_{m_p/m_s} = \frac{Gm_sm_p}{\rho^3}(-\boldsymbol{\rho}) \tag{11b}$$

Eq.(10) thus becomes

$$\ddot{\boldsymbol{\rho}} = \frac{Gm}{\eta^3}\boldsymbol{\eta} - \frac{Gm_s}{\rho^3}\boldsymbol{\rho} \tag{12}$$

- We thus have

$$\ddot{\boldsymbol{\eta}} = \ddot{\mathbf{R}} - \ddot{\boldsymbol{\rho}} \sim \text{ inertial acceleration of } m \text{ relative to } m_p \tag{13}$$

Putting together Eqs.(13), (12) and (6),

$$\ddot{\boldsymbol{\eta}} = -\frac{Gm_p}{\eta^3}\boldsymbol{\eta} - \frac{Gm_s}{R^3}\mathbf{R} - \frac{Gm}{\eta^3}\boldsymbol{\eta} + \frac{Gm_s}{\rho^3}\boldsymbol{\rho}$$

$$= -\frac{G(m_p+m)}{\eta^3}\boldsymbol{\eta} - Gm_s\left(\frac{\mathbf{R}}{R^3} - \frac{\boldsymbol{\rho}}{\rho^3}\right) \tag{14}$$

Rearranging Eq.(14) a little more,

$$\ddot{\boldsymbol{\eta}} = -\frac{Gm_p}{\eta^3}\left(1 + \frac{m}{m_p}\right)\boldsymbol{\eta} - \frac{Gm_s}{R^3}\left(\mathbf{R} - \left(\frac{R}{\rho}\right)^3\boldsymbol{\rho}\right) \tag{15}$$

Now, returning to the geometry of Eq.(1), Eq.(15) transforms to

$$\ddot{\boldsymbol{\eta}} = \underbrace{-\frac{Gm_p}{\eta^3}\left(1 + \frac{m}{m_p}\right)\boldsymbol{\eta}}_{\mathbf{a}_p} - \underbrace{\frac{Gm_s}{R^3}\left(\boldsymbol{\eta} + \left(1 - \left(\frac{R}{\rho}\right)^3\right)\boldsymbol{\rho}\right)}_{\mathbf{a}_{d_s}} \tag{16}$$

Following the same line of reasoning as for Eqs.(7), we have characterized the first term above as the "primary acceleration" and the second terms as the "secondary acceleration". The reason for this nomenclature is that we are now considering the motion of m relative to m_p. Therefore, the influence of m_p is viewed upon as the primary effect and that of m_s as the disturbance.

- Please note that the classification of primary and secondary accelerations are *just names*! There are no approximations and/or ignored terms anywhere. To summarize, the primary and disturbing accelerations on m as viewed from the intermediate object m_p are

$$\mathbf{a}_p = -\frac{Gm_p\left(1+\frac{m}{m_p}\right)}{\eta^3}\boldsymbol{\eta} = \text{"primary"} \tag{17a}$$

$$\mathbf{a}_{d_s} = -\frac{Gm_s}{R^3}\left(\boldsymbol{\eta}+\left(1-\frac{R^3}{\rho^3}\right)\right)\boldsymbol{\rho} = \text{"secondary'} \tag{17b}$$

- It is now time to step in and make some approximations. An obvious one is the following: $1+m/m_p \approx 1$. A slightly less obvious one is the following:

$$1 - \left(\frac{R}{\rho}\right)^3 \approx 0 \tag{18}$$

The above approximation follows from our premise that the SOI is expected to be much smaller than R. In other words, the distance between m_s and m_p is approximately the same as the distance between m_s and m. This was also captured by Eq.(3). Under these approximations, magnitudes of the primary and secondary accelerations of m *as viewed from* m_p can be written as:

$$a_p \approx \frac{Gm_p}{\eta^2} \tag{19a}$$

$$a_{d_s} \approx \frac{Gm_s\eta}{R^3} \tag{19b}$$

And their ratio is,

$$\frac{a_{d_s}}{a_p} = \frac{m_s}{m_p}\left(\frac{\eta}{R}\right)^3 \tag{20}$$

- Let us take stock. We have looked at the motion of the small object m from two perspectives:

  a. The motion of m as *primarily* influenced by m_s and *perturbed* by m_p, resulting in acceleration classification as a_s and a_{d_p}.

  b. The motion of m as *primarily* influenced by m_p and *perturbed* by m_s, resulting in acceleration classification as a_p and a_{d_s}.

It is now time to compare these two viewpoints and thereby define the sphere of influence.

- Laplace argued that inside the SOI of a planet, the ratio of solar disturbance (a_{d_s}) to planetary influence (a_p) is *less* than the ratio of planetary disturbance (a_{d_p}) to solar influence (a_s). I.E., *inside the SOI*,

$$\frac{a_{d_s}}{a_p} < \frac{a_{d_p}}{a_s} \qquad \text{(inside SOI)} \tag{21}$$

From Eqs.(9) and (20),

$$\frac{m_s}{m_p}\left(\frac{\eta}{R}\right)^3 < \frac{m_p}{m_s}\left(\frac{R}{\eta}\right)^2 \tag{22}$$

Now, *on* the surface of the sphere of influence, the two ratios above are the same. Thus at $\eta = R_{SOI}$,

$$\frac{m_s}{m_p}\left(\frac{R_{SOI}}{R}\right)^3 = \frac{m_p}{m_s}\left(\frac{R}{R_{SOI}}\right)^2 \tag{23}$$

Now, from Eq.(3), $R \approx \rho$. Thus we get

$$R_{SOI}^5 = \left(\frac{m_p}{m_s}\right)^2 \rho^5 \tag{24}$$

or,

$$\boxed{R_{SOI,\text{ Laplace}} \triangleq \left(\frac{m_p}{m_s}\right)^{2/5} \rho} \tag{25}$$

where ρ is the distance between m_s and m_p.

❣ **Example** What is the size of the Earth's SOI with respect to the Sun?

We have, $m_p = m_\oplus = 5.974 \times 10^{24}\ kg$; $m_s = m_\odot = 1.989 \times 10^{30}\ kg$. Also, $\rho = 1\ AU$ ($\approx 1.5 \times 10^8$ km). Thus, $R_{SOI,\oplus/\odot} \underset{\text{Eq.(25)}}{=} 9.27 \times 10^5\ km \approx 145$ Earth radii. Fig.(3) shows this pictorially.

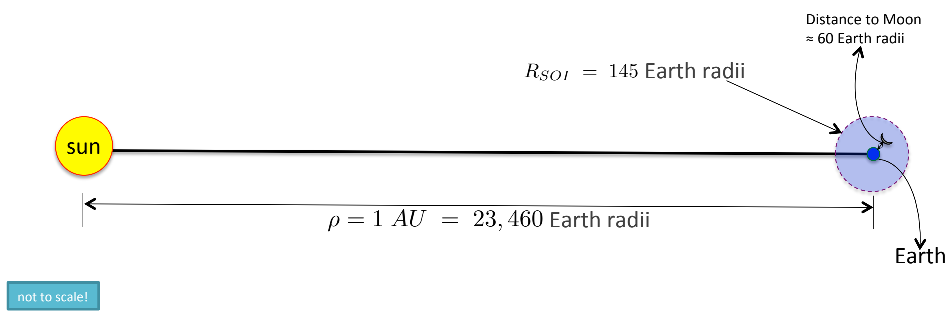

Figure 3: Earth's sphere of influence relative to the Sun.

The following points can be made:

- Our intuition $R_{SOI}/\rho \ll 1$ was correct, because in this example,

$$\frac{R_{SOI,\oplus/\odot}}{\rho} = \frac{145}{23460} \sim 0.006 \sim 0.6\% \tag{26}$$

- The moon (approximately 60 Earth radii from the Earth's center) *lies well within* the sphere of influence of Earth relative to the Sun. This makes sense, after all, it is *our* moon.

❣ **Example** What is the size of the Mars' SOI with respect to the Sun?

Using the numbers for Mars from an online resource,

$$R_{SOI,♂/\odot} = \left(\frac{6.364 \times 10^{23}}{1.989 \times 10^{30}}\right)^{2/5} \times 1.5237\ AU = 5.77 \times 10^5\ km \approx 170\ ♂ \text{ radii} \tag{27}$$

Since Mars is even farther from the Sun than Earth, the approximation of Eq.(3) is even better from it than Earth.

❣ **Example** What is the size of our moon's SOI relative to the Earth?

This is a very interesting study. Note that here, we completely ignore the sun. The two "dominant objects" of concern are the Earth and its moon. Thus, $\rho \approx 384,400\ km$, replace m_s by $m_\oplus = 5.974 \times 10^{24}$ kg and replace m_p with $m_{\leftmoon} = 7.348 \times 10^{22}\ kg$. We get $R_{SOI,\leftmoon/\oplus} = 66,200\ km \approx 10.4$ Earth radii, or, approximately 38 moon radii. Clearly, the moon's SOI relative to the Earth *appears to be* fairly small.

However, recall that absolute numbers mean nothing in the context of the sphere of influence. How small really is the region inside which the moon can be assumed to be the dominant force despite the presence of the Earth? Looking at the ratio R_{SOI}/ρ, we see that

$$\frac{R_{SOI,\leftmoon/\oplus}}{\rho_{\leftmoon/\oplus}} = \frac{66200}{384400} \approx 0.1722 = 17.2\% \tag{28}$$

The above estimate suggests that the distance between the Earth and moon (ρ) is not large enough to *cleanly* decouple their influence on the spacecraft. There is a significant region where both the Earth and moon will have a sizable influence on the spacecraft and a patched conic type of approach, which depends on decoupling the 3-body problem into three two-body problems will be a bad approximation!

Moral of the story: Design of a lunar mission is more difficult than the design of a mission to Mars! Simplifying assumptions that come naturally to the latter do not apply to the former and a much more difficult, coupled, three body problem must be solved. This is shown pictorially in Fig.(4).

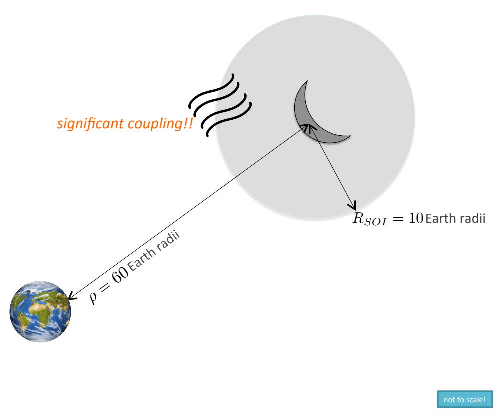

Figure 4: Moon's sphere of influence relative to the Earth.

Mission Design with Patched Conics

As stated earlier, interplanetary mission design via patched conics involves three phases: a departure hyperbola, a cruise ellipse and an arrival hyperbola. Of these, the cruise ellipse is designed first; following which the two hyperbolas are found and patched at the either end points of the heliocentric transfer ellipse (see Fig.(1)).

Cruise Ellipse: A Simplistic Approach

Design of the cruise ellipse is a complex task because not only must we transfer the spacecraft from the Earth's orbit to the orbit of the target planet, the latter must be present to meet the spacecraft when it gets there! Clearly, it is of no use if the spacecraft arrives at its supposed destination and the target planet is somewhere else in its orbit at the time of arrival. In other words, we must account for the motion of the Earth and the target planet in their respective orbits so that we may properly time our arrival at the target. In this section, we will employ the simplest possible method for designing the cruise phase: via a Hohmann-transfer. Of course in order to do so, we must assume the following:

a.) The Earth and the target planet's orbits are circular.

b.) The Earth and target planet's orbits are co-planar.

It is interesting to note that the above assumptions are actually not very far from the truth. The problem with this simplistic approach is something else, as we will soon see.

- Fig.(5) illustrates the design of a cruise ellipse via Hohmann transfer. Point A shows the location of the Earth at the time of departure (launch). Point B shows the location of Mars at the time of arrival. Point C shows the location of Mars at launch. This point is obtained by *backtracking* Mars from point B over the time it takes for the spacecraft to go from A to B. The angular separation between Earth and Mars at the time of launch is given by the angle ϕ and represents the *only* configuration at which a Mars mission can be initiated using a Hohmann transfer. Clearly, if the configuration is even marginally off, a Hohmann transfer is not possible because in a Hohmann transfer, the transfer angle must be 180 deg.

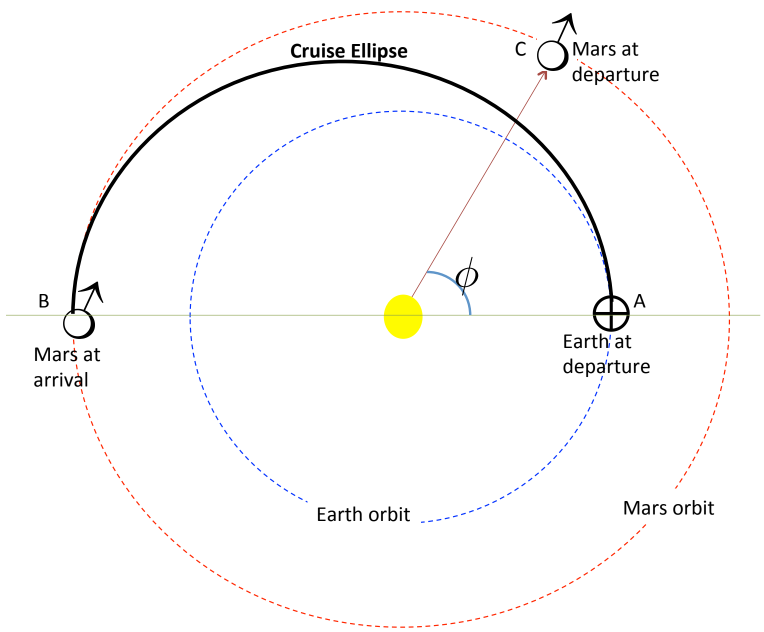

Figure 5: Design of the cruise ellipse via a heliocentric Hohmann transfer.

- We have the following characteristics of the transfer ellipse:

$$a_t = \frac{R_\oplus + R_♂}{2} \tag{29}$$

where a_t is the semi-major axis of the transfer ellipse. Whereby, the period is

$$P_t = 2\pi\sqrt{\frac{a_t^3}{\mu_\odot}} \tag{30}$$

where, $\mu_\odot$ is the gravitational constant of the sun ($= GM_\odot = 1.3271244 \times 10^{20}$). The travel time on the transfer ellipse is: $P_t/2$ (about 260 days).

- We would like to look closer at the "launch alignment" that makes this Hohmann-transfer type mission possible. The phase angle between points B and C is $(\pi - \phi)$, where ϕ is the phase between $\oplus$ and $\male$ at launch. The angular speed of Mars in its orbit is

$$n_{\male} = \frac{2\pi}{P_{\male}} = \sqrt{\frac{\mu_{\odot}}{R_{\male}^3}} \tag{31}$$

Now, the time elapsed in going from point C to B is $P_t/2$, as found above. Therefore, employing the simple "speed× time = distance" formula (riding the circular orbit assumption), we get

$$n_{\male}\frac{P_t}{2} = (\pi - \phi) \tag{32}$$

Or,

$$\phi = \pi - n_{\male}.\frac{2\pi}{2n_t} \qquad \text{(where, } n_t = \frac{2\pi}{P_t}\text{)} \tag{33}$$

Thus

$$\boxed{\phi = \pi\left(1 - \frac{n_{\male}}{n_t}\right) = \pi\left(1 - \frac{P_t}{P_{\male}}\right)} \tag{34}$$

Clearly, the phase separation between Earth and Mars must be exactly ϕ as found above at the time of launch. Only under this alignment of the two planets will the Hohmann transfer approach work. The phase separation is a constant and given by Eq.(34).

- The question is: how often does this alignment occur? I.E. if today is the day Earth and Mars line up as shown in Fig.(5), thus making a Hohmann transfer possible; when will such an opportunity arise again?

It turns out this is a fairly simple computation, given our assumption of circular orbits (which is fairly accurate). The relative speed between Earth and Mars is:

$$n_{\male/\oplus} = n_{\oplus} - n_{\male} \tag{35}$$

(both objects are in prograde orbits around the sun), where, $n_{\male} = \sqrt{\frac{\mu_{\odot}}{R_{\male}^3}}$ and $n_{\oplus} = \sqrt{\frac{\mu_{\odot}}{R_{\oplus}^3}}$. Now, the current configuration is ϕ and the desired final configuration is $(2\pi + \phi)$, i.e. a repeat of the current alignment! Thus, again using the "distance = speed × time" equation, we get:

$$(\phi + 2\pi) - \phi = n_{\male/\oplus}T_{syn} = (n_{\oplus} - n_{\male})T_{syn} \tag{36}$$

where, T_{syn} is the so-called *synodic period*, or the waiting time between feasible planetary alignments allowing a Hohmann transfer. Thus we have,

$$T_{syn} = \frac{2\pi}{(n_{\oplus} - n_{\male})} \tag{37}$$

But, $n_{\oplus} = 2\pi/P_{\oplus}$ and $n_{\male} = 2\pi/P_{\male}$. Thus

$$\boxed{T_{syn,\oplus,\male} = \frac{P_{\oplus}P_{\male}}{(P_{\male} - P_{\oplus})}} \tag{38}$$

Earth's period is 1 year and that of Mars is 1 year and 321.7 days. Thus, $T_{syn,\oplus,\male} = 778$ days.

- For two planets $P1$ and $P2$ in general, the synodic period is

$$T_{syn,P1,P2} = \frac{P_{P1}P_{P2}}{|P_{P1} - P_{P2}|} \tag{39}$$

- We come to the following conclusion. The Hohmann-transfer requires a very special alignment of planets to occur for initiation of the mission, which translates to a virtually vanishingly small launch window. If the opportunity is missed (can happen due to bad weather for example), one must wait 778 days to launch another mission to Mars. Clearly, this is not acceptable and this approach is not viable for mission design. A more general approach is needed, one in which the transfer arc can be less or more than 180 deg. You already are equipped with the necessary toolkit to design such a transfer: namely the Lambert problem solver.

Cruise Ellipse: Lambert's Problem

Interplanetary mission design is an iterative process. We like the Hohmann approach because it is optimal in terms of Δv. But it is undesirable in the sense that it provides an almost non-existent launch opportunity. Therefore, we wish to relax the design parameters somewhat, and allow for variation in launch and arrival dates. This opens the launch window a little broader, but entails that the transfer ellipse is no longer the optimal Hohmann ellipse.

Thus mission design proceeds as follows: pick a date of launch and arrival close to the Hohmann opportunity. Obtain the Δv's associated with these dates (actually shown as a $C3$ value: recall hyperbolas). The computed $C3$ is shown on a plot along with the launch and departure date. Then a different pair of launch and departure dates are picked and the analysis is repeated, until a graph is obtained that shows the required $C3$ (a descriptor of mission feasibility) as a function of the launch and departure dates. The $C3$ plot for the 2005 Mars launch opportunity is shown in Fig.(6). This figure is called a "porkchop" plot (probably because of the shape of the $C3$ contours). The outer contours have a high $C3$ value and thus may be unfeasible. Depending on the capability of the rockets and onboard propellant available, a launch window can be defined as the set of available launch dates on which the $C3$ required to execute the mission is feasible.

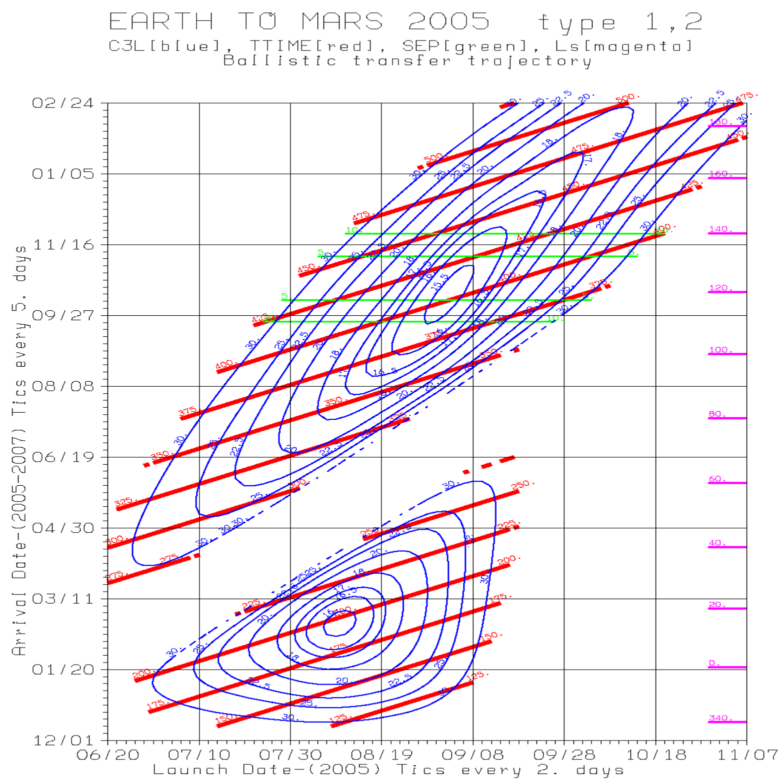

Figure 6: A Mars porkchop: 2005 launch opportunity. Source: wikipedia

For every pair of launch and arrival dates shown on the porkchop (except the pair that corresponds to Hohmann transfer), a Lambert's problem must be solved. We will now discuss this procedure.

– The first step is to pick a launch and arrival date, namely t_1 and t_2 respectively.

– **Time of Flight: Julian dates.** Once the launch and arrival dates have been selected, the time of flight can technically be obtained. However, it is a tedious task to compute travel time from calendar dates in mm/dd/yyyy format. There exists a convenient numbering system that assigns a unique real number to any date, called its *Julian date*. This number is a monotonically increasing function of time. In the Julian date system, the time between any two dates can be computed as a simple subtraction.

By definition, the Julian date is the number of days since *noon UT of Jan 1, 4713 B.C.*, where UT stands for universal time ($\sim$ GMT). Let the calendar entry of the date of interest be d (day), m (month) and y (year). Then, its Julian date J_0 is defined as

$$J_0 \;=\; 367y - \text{INT}\left\{\frac{7\left[y + \text{INT}\left(\frac{m+9}{12}\right)\right]}{4}\right\} \;+\; \text{INT}\left(\frac{275m}{9}\right) \;+\; d \;+\; 1721013.5 \qquad (40)$$

where, "INT" is the integer function: it rounds a real number <u>down</u> to the closest integer. E.g., INT(4.2) = 4, INT(4.5) = 4, INT(4.7) = 4. The inbuilt MATLAB®function for this is called "floor". The Julian date J_0 corresponds to 0000 hrs of the date of interest. To adjust for the current time (expressed in UT), the following modification is made:

$$JD(y, m, d, UT) \;\triangleq\; J_0(y, m, d) \;+\; \frac{UT}{24} \qquad (41)$$

The above equations for Julian date are valid for $1901 \leqslant y \leqslant 2099$, $1 \leqslant m \leqslant 12$, $1 \leqslant d \leqslant 31$ and $0 \leqslant UT \leqslant 24$.

❢ **Example** Determine the equivalent Julian date for April 30, 2014, 5:00:00 PM local Gainesville time.
Solution: Here, $y = 2014$, $m = 4$, $d = 30$. Thus,

$$J_0 \;=\; 367y - \text{INT}\left\{\frac{7\left[y + \text{INT}\left(\frac{m+9}{12}\right)\right]}{4}\right\} \;+\; \text{INT}\left(\frac{275m}{9}\right) \;+\; d \;+\; 1721013.5 \;=\; 2456777.5 \quad (42)$$

Adjustment for time: In terms of UT, 5:00:00 PM USA/Eastern $\equiv$ 9:00:00 PM UT $\equiv$ 21:00:00 hrs UT $\equiv 21 + 0/60 + 0/3600 = 21.00$ hrs. Thus,

$$JD(2014, 04, 30, 21:00:00UT) \;=\; J_0 \;+\; \frac{21.00}{24} \;=\; 2456778.375 \qquad (43)$$

It is easy to see that the concept of Julian date greatly facilitates the computation of time of flight. Let the Julian dates of launch and arrival times be JD_L and JD_A respectively. Then,

$$TOF \;=\; JD_A \;-\; JD_L \qquad (44)$$

– **Ephemeris information.** Given the launch and arrival dates, the next step is to determine the planetary locations at the these dates. This is done using a so-called *Ephemeris calculator*. An ephemeris calculator does something fairly straightforward: using a date and time as input (perhaps in JD format), it spits out the inetial position and velocity vectors of an object, e.g. the heliocentric states of a planet. You may write your own Ephemeris code by solving the two-body problem - keep in mind you will need state0measurements at some point in time for use as initial conditions. With this reference, you can predict the future states at desired times. Of course, your code will be simplistic because you wouldn't account for non-Keplerian perturbations. There are numerous accurate Ephemeris tools publicly available, e.g. the JPL Horizons Ephemeris calculator @ http://ssd.jpl.nasa.gov/horizons.cgi.

– We now have all the information available to set up the Lambert's problem for mission design. As mentioned above, let the launch and arrival dates be depicted by JD_L and JD_A respectively.

From the Ephemeris calculator, let the obtained the position of Earth at launch be $\mathbf{R}_\oplus = \mathbf{R}_1$ and the position of the target planet (say Mars) at arrival be $\mathbf{R}_♂ = \mathbf{R}_2$. Also let the corresponding velocity vectors be $\mathbf{v}_\oplus$ and $\mathbf{v}_♂$ respectively. Using $\mathbf{R}_1$, $\mathbf{R}_2$ and TOF as input, design the transfer ellipse using the Lambert's sovler developed in the notes on *Preliminary Orbit Determination*.

Lets do this using an actual example for a real Mars mission in the 1996 launch window.

❣ **Example** Consider a Mars mission set for launch on 11/7/1996, 0000 hrs UT and arrival on 09/12/1997 at 0000 hrs UT. The mission begins on a circular parking orbit of altitude 180 km above the Earth. It is desired to place the spacecraft in an elliptic mapping orbit around Mars of period 48 hrs and a close approach of 300 km altitude.

In this part, we will only design the cruise phase of the mission, i.e. the heliocentric transfer ellipse. We have:

$$\text{Launch: } 11/7/1996, 0000 \text{ hrs } UT \implies JD_L \underset{\text{Eq.(40)}}{=} 2450394.5 \tag{45}$$

$$\text{Arrival: } 9/12/1997, 0000 \text{ hrs } UT \implies JD_A \underset{\text{Eq.(40)}}{=} 2450703.5 \tag{46}$$

Thus, time of flight:

$$TOF = JD_A - JD_L = 309 \text{ days} \tag{47}$$

Given the launch and arrival dates, the following ephemeris data was obtained from JPL/Horizons:

Earth @ launch:

$$\mathbf{R}_\oplus = \mathbf{R}_1 = [1.05 \times 10^8,\ 1.046 \times 10^8,\ 988.3]\ km \tag{48a}$$

$$\mathbf{v}_\oplus = [-21.52,\ 20.99,\ 1.32 \times 10^{-4}]\ km/s \tag{48b}$$

And,

Mars @ arrival:

$$\mathbf{R}_♂ = \mathbf{R}_2 = [-2.08 \times 10^7,\ -2.18 \times 10^8,\ -4.06 \times 10^6]\ km \tag{49a}$$

$$\mathbf{v}_♂ = [25.04,\ -0.22,\ -0.62]\ km/s \tag{49b}$$

We can now use the radius vectors $\mathbf{R}_1$ and $\mathbf{R}_2$ from Eqs.(48a) and (49a) respectively and TOF from Eq.(47) to solve the Lambert's problem for the transfer ellipse. The steps are laid out below.

- Transfer angle during cruise:

$$\Delta\theta = \cos^{-1}\left(\frac{\mathbf{R}_1 \cdot \mathbf{R}_2}{R_1 R_2}\right) = 2.4492\ rad = 140.33 \deg \tag{50}$$

  Check however $\text{sign}(\sin\Delta\theta) = \text{sign}[(\mathbf{R}_1 \times \mathbf{R}_2)_z] = \text{sign}(-2.0714 \times 10^{22}) = -1$. Thus we must correct the transfer angle to $\Delta\theta \to 2\pi - \Delta\theta = 3.8340\ rad \equiv 219.671$ deg.

- Other known data: $R_1 = \|\mathbf{R}_1\| = 1.4821 \times 10^{11}\ m$, $R_2 = \|\mathbf{R}_2\| = 2.1903 \times 10^{11}\ m$. Time of flight: $\Delta t = 309 * (24 * 3600) = 2.66976 \times 10^7\ s$. Also, we have the constants K_1 and K_2:

$$K_1 = \mu_\odot(1 - \cos\Delta\theta) = 2.3483 \times 10^{20} \tag{51a}$$

$$K_2 = \sqrt{\frac{\mu_\odot R_1 R_2}{K_1}} \sin\Delta\theta = -8.6512 \times 10^{10} \tag{51b}$$

- Next, execute Newton's iterations to determine $z\ (= \alpha\chi^2)$ using a universal threshold of $\epsilon = 10^{-12}$. The evolution is shown in Table.(1). At the end, $z = \alpha\chi^2 = 14.8190$.

Table 1: Newton-Raphson Iteration Evolution for Lambert's Problem: Cruise Ellipse

Iteration # (k)	Correction: Δz^k	Approximation: $z^{(k)}$
0	-	0 (initial guess)
1	3.7634e+01	3.7634e+01
2	-6.0914e-01	3.7025e+01
3	-8.0829e-01	3.6216e+01
4	-1.0712e+00	3.5145e+01
5	-1.4168e+00	3.3728e+01
6	-1.8663e+00	3.1862e+01
7	-2.4353e+00	2.9427e+01
8	-3.1022e+00	2.6324e+01
9	-3.7187e+00	2.2606e+01
10	-3.8438e+00	1.8762e+01
11	-2.8283e+00	1.5934e+01
12	-1.0194e+00	1.4914e+01
13	-9.4571e-02	1.4820e+01
14	-7.1265e-04	1.4819e+01
15	-3.9957e-08	1.4819e+01
16	$\boxed{1.3955e-14}$: **STOP!!**	1.4819e+01

- At the converged value of z, various functions evaluated are: $C(z) = 0.1187$, $S(z) = 0.0789$, $Y(z) = U_2(a,z) = 3.2482 \times 10^{11}$. Thus, we get

$$a = \frac{Y(z)}{zC(z)} = 1.8460 \times 10^{11}\ m = 1.2306\ AU \tag{52}$$

Also, we have the angular momentum:

$$h = \sqrt{\frac{K_1 R_1 R_2}{U_2(a,\hat{E})}} = 4.8443 \times 10^{15}\ m^2/s^2 \tag{53}$$

- We are now ready to evaluate the Lagrange coefficients for this problem, which turn out to be: $F = -1.1916$, $G = -4.2800 \times 10^6$, $\dot{F} = 9.9153 \times 10^{-8}$ and $\dot{G} = -0.4831$.

- Substitution of the Lagrange parameters into the $F - G$ framework gives:

$$\mathbf{v}_1 = [-24.397,\ 21.813,\ 0.9483]\ km/s \tag{54a}$$
$$\mathbf{v}_2 = [22.196,\ -0.1655,\ -0.4580]\ km/s \tag{54b}$$

- Pick the pair $(\mathbf{r}_1, \mathbf{v}_1)$ to determine the orbit. You could also have used the pair $(\mathbf{r}_2, \mathbf{v}_2)$. The elements of the transfer ellipse are:

$$a = \frac{-\mu}{2\varepsilon} = 1.846 \times 10^{11}\ km = 1.2306\ AU \tag{55a}$$

$$\begin{aligned}
e &= \sqrt{1 - p/a} \;=\; 0.205 && (55\text{b})\\
i &= \cos^{-1}(\hat{\mathbf{i}}_h(3)) \;=\; 1.66\,\text{deg} && (55\text{c})\\
\Omega &= \tan^{-1}(\hat{\mathbf{i}}_h(1)/(-\hat{\mathbf{i}}_h(2)) \;=\; 44.88\,\text{deg} && (55\text{d})\\
\omega &= \tan^{-1}(\hat{\mathbf{i}}_e(3)/\hat{\mathbf{i}}_y(3)) \;=\; 19.67\,\text{deg} \quad \text{and,} && (55\text{e})\\
f_1 &= 340.34\,\text{deg} \quad \text{(careful with quadrant)} && (55\text{f})
\end{aligned}$$

Departure Hyperbola Design

The geometry of departure from Earth is shown in Fig.(7). The parking orbit is shown in green from which the point of departure is A. As far as the hyperbola is concerned, the edge of the SOI is as good as ∞, because the conic is centered at the Earth. Therefore, at the patching point $P1$ (which is also the starting point for the transfer ellipse), the spacecraft velocity on the Earth centered departure hyperbola is essentially $\mathbf{v}_{\infty,DH}$.

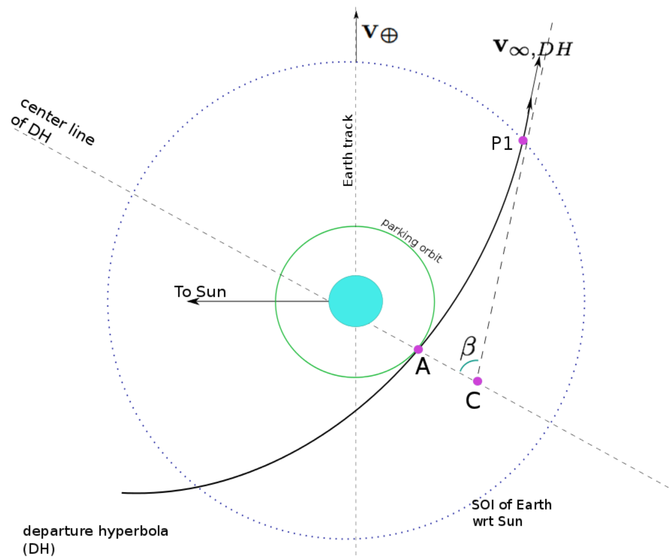

Figure 7: An illustration of the *departure hyperbola*.

- Also shown in the above figure is the heliocentric track of Earth and its velocity vector with respect to the Sun. The geometry of the velocity vectors at the patching point is shown in Fig.(8). The various vectors in this figure can be described as follows:
  - $\mathbf{v}_1$: velocity vector of the spacecraft with respect to the sun on the cruise ellipse at $P1$. This vector can also be written as $\mathbf{v}_{sc/\odot,P1}$.
  - $\mathbf{v}_\oplus$: this is the velocity vector of the Earth with respect to the sun at the time instant shown, or $\mathbf{v}_{\oplus/\odot}$.
  - $\mathbf{v}_{\infty,DH}$: the velocity vector of the spacecraft with respect to the Earth at the patching point $P1$. We can write it as $\mathbf{v}_{sc/\oplus,P1}$.
- Adding relative velocities, we get that

$$\mathbf{v}_{sc/\odot,P1} = \mathbf{v}_{sc/\oplus,P1} + \mathbf{v}_{\oplus/\odot} \tag{56}$$

or,

$$\mathbf{v}_1 = \mathbf{v}_\oplus + \mathbf{v}_{\infty,DH} \tag{57}$$

- Note that $\mathbf{v}_\oplus$ is *known* (from Ephemeris data) and the vector $\mathbf{v}_1$ we just found as part of the solution to the Lambert's problem. Thus

$$\mathbf{v}_{\infty,DH} = \mathbf{v}_1 - \mathbf{v}_\oplus \tag{58}$$

  The above is the *excess velocity vector* of the spacecraft on the departure hyperbola. It magnitude is simply $v_{\infty,DH} = \|\mathbf{v}_{\infty,DH}\|$. Following with the example problem above, we get:

$$\mathbf{v}_{\infty,DH} \sim \mathbf{v}_{\infty,\text{depart}} = [-2.876,\ 0.825,\ 0.949]\ km/s \tag{59}$$

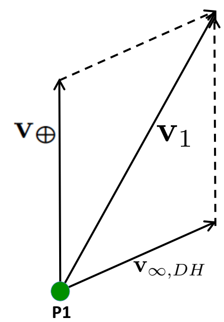

Figure 8: Geometry of velocity vectors at patching point P1.

Therefore, $v_{\infty,\text{depart}} = 3.139$ *kmps*. This information is enough to help us compute the energy of the departure hyperbola: simply apply the vis-viva equation at the edge of the SOI (which is almost infinity):

$$\varepsilon_{DH} = \underbrace{\frac{v_{SOI}^2}{2}}_{\approx \frac{v_\infty^2}{2}\ (?)} - \underbrace{\frac{\mu_\oplus}{R_{SOI,\oplus/\odot}}}_{\approx 0\ (?)} \tag{60}$$

It is time to take a step back: *how good really is the approximation that at the edge of the SOI, we are effectively at infinity on the geocentric departure hyperbola?* There are at least two ways to get an estimate: (a) determine the true anomaly at the edge of the SOI (recall $R_{SOI,\oplus/\odot} \approx 145$ Earth radii) and match it with f_∞; (b) compute the potential energy term in the vis-viva equation shown above and assess its influence on the evaluation of the semi-major axis of the hyperbola.

The first of these methods is not yet feasible because the eccentricity of the orbit is not known yet. Following method (b), we see that

$$|\text{Potential Energy @ } R_{SOI}| = \frac{\mu_\oplus}{R_{SOI,\oplus/\odot}} = \frac{3.986004 \times 10^{14}}{145 \times 6378.14 \times 10^3} \approx 4.31 \times 10^5 \text{ !!} \tag{61}$$

Clearly, the potential energy is not zero, like we dismissively assumed it to be in Eq.(60)! However, its absolute magnitude is of no significance: we must answer the following questions: (i) how does the potential energy compare with the kinetic energy (i.e. $v_\infty^2/2$ term) and (ii) by how much would the estimate of the semi-major axis change if we included the potential energy term? Let us examine both these questions:

i.) Comparison to kinetic energy (for the example problem): We have, $v_\infty^2/2 = 4.925 \times 10^6$, i.e.

$$\frac{\text{Potential Energy}}{\text{Kinetic Energy}} = \frac{\mu_\oplus/R_{SOI,\oplus/\odot}}{v_\infty^2/2} = 0.0875 \sim 8.75\% \tag{62}$$

Based on the above metric, the "infinity approximation" is good but not great. Note that the above estimate *applies only to the present example.* The estimate of the potential energy is universal (depends only on the size of Earth's SOI) but the kinetic energy depends on the particular mission.

ii.) Influence on computation of semi-major axis: If we ignore the potential energy in comparison to the kinetic energy, we get

$$a_{1,DH} = -\frac{\mu_\oplus}{v_{\infty,DH}^2} = -4.0467 \times 10^7\ m \tag{63}$$

On the other hand, if we include the influence of the potential energy term for computation of a, we get

$$a_{2,DH} = -\frac{\mu_\oplus}{2(v_{\infty,DH}^2/2 - \mu_\oplus/R_{SOI,\oplus/\odot})} = -4.4348 \times 10^7\ m \tag{64}$$

Again, $|a_2 - a_1|/a_2 \ = \ 0.0875 \sim 8.75\%$!!

Obviously, the above numbers are enough reason to feel a slight heartburn. We have discovered that our "infinity assumption" is not really an exceptionally good approximation, it is just about OK.

You *could argue* that there is a way around the above problem: simply do not assume that $\mathbf{v}_{sc/\oplus,P1}$ is the same as $\mathbf{v}_{\infty,DH}$. The geometry of the velocity vectors (Fig.(8)) still holds and we do have an estimate of the spacecraft's potential energy at the edge of Earth's SOI (Eq.(61)). So why not simply use both the potential and kinetic energy terms to estimate the total energy of the hyperbola (and subsequently its semi-major axis)? This argument appears enticing but is flawed. Note that the edge of Earth's SOI relative to the Sun is a "high coupling" zone, where both the Sun's and Earth's gravitational fields are about equally important. Therefore no matter what we do in this region, our computations will be erroneous so long as we stick to the two-body model, irrespective of whether the model involves the spacecraft and Earth or the spacecraft and Sun. It would have been nice if our decoupling were "cleaner", i.e. the edge of the SOI were really the *infinity* for the departure hyperbola - then we could be justified in saying that the spacecraft had well and truly left the confines of Earth. Unfortunately, this is not true as is reflected in the 8.75% anomaly computed above. Be careful however: this number is valid only for the current example problem and would be different for a different mission. This anomaly is unavoidable in the current method and we must correct for it in the next level of mission design (not part of this course).

Conclusion: To be consistent with our philosophical understanding of the sphere of influence, we will continue to assume that $\mathbf{v}_{sc/\oplus,P1} \ = \ \mathbf{v}_{\infty,DH}$. The argument is flawed, but consistent with the design model. Thereby, Eq.(63) must be preferred over Eq.(64).

- There is one other piece of information we have about the departure hyperbola: namely its periapsis radius - it is the same as the radius of the parking orbit (see Fig.(7)). In other words, the departure point (A) is the periapsis of the hyperbola. Mathematically, $r_A \ = \ r_{p,DH} \ = \ r_{\text{park}}$. We can use vis-viva to determine the speed on the hyperbola at the departure point:

$$\frac{v_{p,DH}^2}{2} \ = \ \varepsilon_{DH} \ + \ \frac{\mu_\oplus}{r_{p,DH}} \tag{65}$$

Using Eq.(60),

$$\frac{v_{p,DH}^2}{2} \ = \ \frac{v_{\infty,DH}^2}{2} \ + \ \frac{\mu_\oplus}{r_{\text{park}}} \tag{66}$$

Or,

$$v_{p,DH}^2 \ = \ \underbrace{v_{\infty,DH}^2}_{=C3_{DH}} \ + \ \frac{2\mu_\oplus}{r_{\text{park}}} \tag{67}$$

where $C3 = v_\infty^2$ is a measure of the excess hyperbolic kinetic energy. In the current example,

$$v_{p,DH} \ = \ \sqrt{C3_{DH} \ + \ \frac{2\mu_\oplus}{r_{\text{park}}}} \ = \ 11.368 \ km/s \tag{68}$$

- Of course, we also know the speed on the parking orbit:

$$v_{\text{park}} \ = \ \sqrt{\frac{\mu_\oplus}{r_{\text{park}}}} \qquad (= 7.7961 \, km/s \text{ in the current problem}) \tag{69}$$

- The eccentricity of the departure hyperbola can be computed as,

$$e_{DH} \ = \ 1 \ + \ \frac{C3_{DH} \, r_{p,DH}}{\mu_\oplus} \qquad (= 1.162 \text{ in the current problem}) \tag{70}$$

- Finally, we estimate the requisite Δv required at departure to transfer the spacecraft from the parking orbit to the departure hyperbola:

$$\Delta v_{\text{depart}} = v_{p,DH} - v_{\text{park}} \tag{71}$$

Or,

$$\boxed{\Delta v_{\text{depart}} = \sqrt{C3_{DH} + \frac{2\mu_\oplus}{r_{\text{park}}}} - \sqrt{\frac{\mu_\oplus}{r_{\text{park}}}}} \tag{72}$$

which for the current problem is $\Delta v_{\text{depart}} = 3.674\ km/s$ (a "mere" 438 m/s more than Δv_{escape}).

- Note: The transition from the departure hyperbola to the cruise ellipse is ***automatic***, i.e. nothing needs to be done at the patching point $P1$. The geometry of Fig.(8) was used *as the boundary condition* to design "just the perfect" hyperbola which patches (almost) perfectly with the cruise ellipse at the sphere of influence. As the Sun takes over beyond the Earth's SOI, the departure hyperbola becomes the cruise ellipse. This is quite elegant when you think about it.

Arrival Hyperbola Design

The final stage of the mission is the arrival hyperbola. Just like for the departure hyperbola, we will use the patching condition on the edge of the target planet's SOI to get the appropriate boundary-conditions at infinity for the incoming hyperbola. Fig.(9) shows the arrival scene. The desired target orbit is shown in green. As shown, the incoming hyperbola is designed so as to be tangential to the target orbit at the former's periapsis (point B). The arrival hyperbola must therefore be designed so that it matches the boundary conditions both at the patching point ($P2$) and the point of intersection with the target orbit (B).

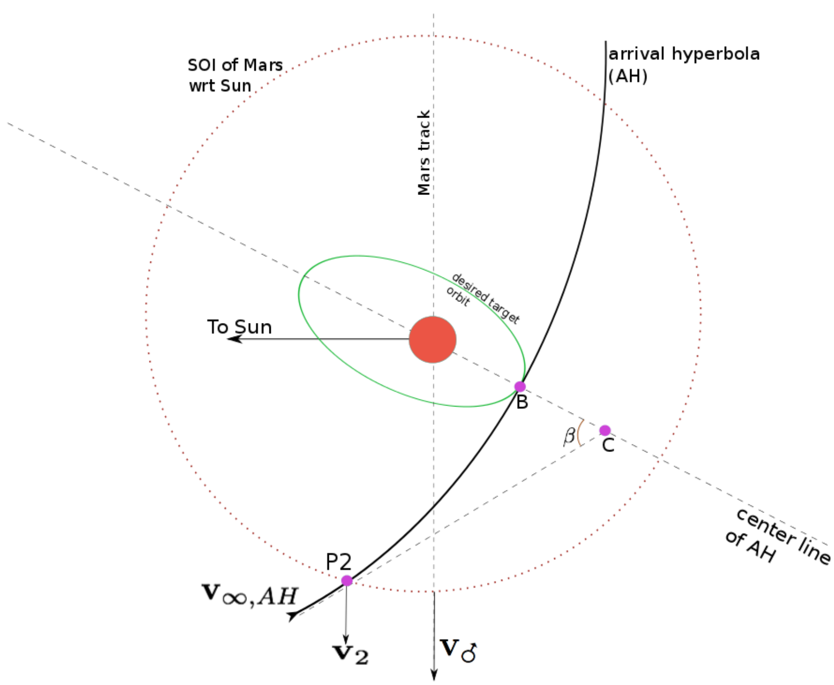

Figure 9: An illustration of the *arrival hyperbola*.

- The geometry of the velocity vectors looks similar to the departure case, and is shown in Fig.(10). A similar trio as in Earth departure exists:

– $\mathbf{v}_2$: velocity vector of the spacecraft with respect to the sun on the cruise ellipse at $P2$. This vector can also be written as $\mathbf{v}_{sc/\odot,P2}$.
– $\mathbf{v}_{♂}$: this is the velocity vector of Mars with respect to the sun at the time instant shown, or $\mathbf{v}_{♂/\odot}$.
– $\mathbf{v}_{\infty,AH}$: the velocity vector of the spacecraft with respect to Mars at the patching point $P2$. We can write it as $\mathbf{v}_{sc/\oplus,P2}$.

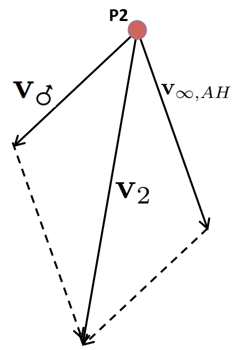

Figure 10: Geometry of velocity vectors at patching point P1.

- Following the algebra of relative velocity vectors,

$$\mathbf{v}_{\infty,AH} \;=\; \mathbf{v}_2 \;-\; \mathbf{v}_{♂} \tag{73}$$

Using $\mathbf{v}_2$ from our solution of the Lambert's problem and $\mathbf{v}_{♂}$ from the ephemeris data, we get

$$\mathbf{v}_{\infty,AH} \;=\; [-2.844,\, 0.0448,\, 0.1616]\; km/s \tag{74}$$

And, $v_{\infty,AH} \;=\; 2.849\; kmps$.

- It is tempting to check for the accuracy of the decoupling assumption for arrival. Recall that $R_{SOI,♂/\odot} \;=\; 5.77 \times 10^5\; km$:

$$\frac{\text{Potential Energy}_{♂SOI}}{\text{Kinetic Energy}_{♂SOI}} \;=\; \frac{\mu_{♂}/R_{SOI,♂/\odot}}{v^2_{\infty,AH}/2} \;=\; 0.0183 \sim 1.83\% \tag{75}$$

Clearly, the above number is much better than what we found for departure! The decoupling is cleaner at arrival and the reason is: Mars is farther from the Sun than Earth. So, the coupling is somewhat weaker to begin with and consequently, the *de*coupling is not surprisingly, cleaner.

- With a significantly cleaner conscience (☺), we can compute the energy of the arrival hyperbola as:

$$\varepsilon_{AH} \;=\; -\frac{\mu_{♂}}{2a_{AH}} \;=\; \frac{v^2_{\infty,AH}}{2} \tag{76}$$

For the example problem, $\varepsilon_{AH} \;=\; 4.0585 \times 10^6\; m^2/s^2$ and $a_{AH} \;=\; -5.2773 \times 10^6\; m$.

- Let us now look at the boundary condition at the point of intersection with the target orbit: we have $r_{p,AH} \;=\; r_{p,\text{target}}$. Let us apply the vis-viva equation to determine $v_{p,AH}$:

$$v^2_{p,AH} \;=\; 2\varepsilon_{AH} \;+\; \frac{2\mu_{♂}}{r_{p,AH}} \tag{77a}$$

$$\;=\; \underbrace{v^2_{\infty,AH}}_{=C3_{AH}} \;+\; \frac{2\mu_{♂}}{r_{p,\text{target}}} \tag{77b}$$

Thus

$$v_{p,AH} = \sqrt{C3_{AH} + \frac{2\mu_♂}{r_{p,\text{target}}}} \tag{78}$$

For our current example, $r_{p,\text{target}} = 300 + 3380 = 3680\ km$. Thus, $v_{p,AH} = 5.598\ km/s$.

- The eccentricity of the incoming hyperbola is

$$e_{AH} = 1 + \frac{C3_{AH}\, r_{p,AH}}{\mu_♂} \qquad (= 1.699 \text{ in the current problem}) \tag{79}$$

- Before we compute the Δv needed to transfer the spacecraft from the arrival hyperbola to the target orbit, we must obtain further characteristics of the latter. Using its given period, we have

$$a_{\text{target}} = \left(\frac{P^2_{\text{target}}\, \mu_♂}{4\pi^2}\right)^{1/3} \tag{80}$$

which amounts to 31,880 km in the current example. Also, the eccentricity of the target orbit is $e_{\text{target}} = 1 - r_{p,\text{target}}/a_{\text{target}} = 0.885$. Also, the speed at periapsis is:

$$v_{p,\text{target}} = \sqrt{2\left(\frac{\mu_♂}{r_{p,\text{target}}} - \frac{\mu_♂}{2a_{\text{target}}}\right)} \tag{81}$$

In the present example, the above speed is 4.683 km/s.

- We have everything available now to compute the required Δv at arrival:

$$\boxed{\Delta v_{\text{arrive}} = (v_{p,AH} - v_{p,\text{target}}) = \sqrt{C3_{AH} + \frac{2\mu_♂}{r_{p,\text{target}}}} - \sqrt{2\left(\frac{\mu_♂}{r_{p,\text{target}}} - \frac{\mu_♂}{2a_{\text{target}}}\right)}} \tag{82}$$

The above burn amounts to 920.7 m/s in the current example.

- The **total mission** Δv for this design is

$$\Delta v_{\text{mission}} = \Delta v_{\text{depart}} + \Delta v_{\text{arrive}} = 4.588\ km/s. \tag{83}$$

- Just like in the departure scenario, the patching at the Mars SOI is automatic, i.e. no burns are needed at that point. By construction, the arrival hyperbola is designed to smoothly (smoother than departure actually: see Eq.(75)) transfer the spacecraft from the realm of the Sun into the regime of Mars.

Congratulations. You just designed your first realistic mission to Mars.